Composites Part B 106 (2016) 190–205

Contents lists available at ScienceDirect

Composites Part B

journal homepage: www.elsevier.com/locate/compositesb

TRM vs FRP jacketing in shear strengthening of concrete members subjected to high temperatures

Zoi C. Tetta [a, *], Dionysios A. Bournas [b]

[a] Department of Civil Engineering, University of Nottingham, NG7 2RD, Nottingham, UK
[b] European Commission, Joint Research Centre (JRC), Directorate for Space, Security & Migration, Safety and Security of Buildings, European Laboratory for Structural Assessment, TP480, Via Enrico Fermi 2749, I-21020, Ispra, VA, Italy

ARTICLE INFO

Article history:
Received 4 July 2016
Received in revised form
1 September 2016
Accepted 8 September 2016
Available online 10 September 2016

Keywords:
Fabrics/textiles
Carbon fibre
Glass fibres
Debonding
High temperature

ABSTRACT

This paper presents the first study on the performance of TRM and FRP jacketing in shear strengthening of reinforced concrete (RC) members subjected to ambient and high temperatures, including both medium-scale rectangular beams and full-scale T-beams. Key parameters investigated on the medium-scale rectangular RC beams include: (a) the matrix used to impregnate the fibres, namely resin or mortar, resulting in two strengthening systems (TRM or FRP), (b) the level of high temperature to which the specimens are exposed (20 °C, 100 °C, 150 °C, 250 °C), (c) the strengthening configuration (side-bonding, U-wrapping and full-wrapping), (d) the number of jacketing layers (2 and 3) and (e) the textile properties (geometry, material). The effectiveness of both non-anchored and anchored TRM jackets in shear strengthening of full-scale T-beams at high temperature was also studied. It is concluded that TRM possess excellent performance as strengthening material at high temperature. TRM jacketing remained very effective in shear strengthening of concrete at high temperature; on the contrary the effectiveness of side-bonding and U-wrapping FRP jacketing was reduced nearly to zero when subjected at temperatures above the glass transition temperature.

1. Introduction and background

The issue of upgrading existing structures has been of great importance over the last decades due to their deterioration; ageing, environmental induced degradation, lack of maintenance or need to meet the current safety design standards (i.e. Eurocodes). Fibre reinforced polymers (FRP) have been widely used as externally bonded (EB) reinforcement of existing structurally deficient structures over the last three decades due to their favourable properties (i.e. high strength to weight ratio, corrosion resistance, ease and speed of application, and minimal change of geometry). However, the FRP strengthening technique entails a few drawbacks mainly associated with the use of epoxy resins. In particular, except from their high costs and their inability to apply on wet surfaces, FRP have very poor performance at high temperature as under loading epoxy resins normally lose their tensile capacity. Therefore, unless protective (thermal insulation) systems are not provided [1,2], the bond capacity at the FRP-concrete interface will be extremely low above the glass transition temperature (T_g). A state-of-the-art review on the fire behaviour of reinforced concrete (RC) members strengthened with FRPs was recently conducted by Firmo et al. [3].

The last decade, a new composite material, namely textile-reinforced mortar (TRM) has been proposed for structural retrofitting [4,5]. TRM combines advanced fibres in form of textiles (with open-mesh configuration) with inorganic matrices, such as cement-based mortars. TRM is a relatively low cost strengthening material, friendly for manual workers and compatible to concrete or masonry substrates material, whereas can be applied on wet surfaces or at low temperatures. The same material can also be found in the literature as FRCM [6]. Bond between TRM or FRCM and concrete substrates has been widely studied [i.e. 7–9]. TRM has been also investigated as a strengthening system of RC elements [10–17] or structures [18] and has been found to be a very promising solution. Selected case studies of actual applications of TRM in the construction field can be found in Ref. [19].

Shear strengthening of RC beams or bridge girders in old RC structures is one of the most common needs when assessing their strength under the current code requirements because of the insufficient amount of shear reinforcement, corrosion of existing shear reinforcement, low concrete strength and/or increased

* Corresponding author.
E-mail address: zoi.tetta@nottingham.ac.uk (Z.C. Tetta).

http://dx.doi.org/10.1016/j.compositesb.2016.09.026

design load. Shear strengthening of RC beams with TRM has been investigated by few researchers [4,20–26]. A variety of parameters has been studied including the performance of TRM versus FRP jackets [4,22,23,26], the number of layers [4,20,22,23,26], the strengthening configuration [21,23], and the end-anchorage of TRM U-jackets in T-beams [20,22,26].

TRM is breathable, non-combustible nor flammable and many researchers have argued that TRM will naturally outperform FRP at elevated temperature or fire. However, research on the performance of TRM systems at elevated temperature or fire and comparison between TRM and FRP at high temperature or fire is extremely limited. This is attributed to the inherent experimental difficulties in the simultaneous application of loading and high temperature, even for medium or small-scale specimens. For this reason, the studies found are focused on either characterising the tensile stress-strain behaviour of TRM as a composite material, or investigating the residual capacity of TRM as a strengthening material of RC members. In specific, Colombo et al. [27] studied the behaviour of TRM at high temperature conducting tensile tests on TRM coupons. The specimens were first exposed to high temperature and after a 2 h stabilization phase, they were cooled down before testing. They concluded that in case of 200 °C, TRM coupons keep their strength, whereas the stress and strain significantly decrease after the exposure of specimens to 400 °C and 600 °C due to deterioration of the textile mesh coating. Al-Salloum et al. [28] studied the effect of high temperature on the residual axial capacity of concrete circular columns strengthened with four different strengthening techniques, namely continuous carbon FRP sheets (CF), carbon FRP strips combined with near surface mounted (NSM) steel bars (CFS/NSM), continuous glass FRP sheets combined with NSM steel bars (GF/NSM) and continuous TRM layers combined with NSM steel bars (TRM/NSM). Based on their results, GF/NSM was the most effective technique at high temperature (300 °C), followed by TRM/NSM, whereas CF and CFS/NSM were the less efficient strengthening techniques in terms of residual axial strength, secant stiffness and peak axial strain.

The only study reported in the literature on TRM versus FRP as strengthening materials at high temperature is that of Bisby et al. [29], who did flexural strengthening of RC beams. In particular, both un-retrofitted and strengthened beams tested up to failure at ambient temperature, whereas their counterpart specimens were tested under sustained load while being exposed to increasing high temperature. In specimens tested at high temperature, the critical-anchorage zones were kept cool (presuming that debonding of heated anchorage zones is prevented through insulation or by mechanical means) and therefore the effect of high temperature on the debonding mechanism of the jacket from the concrete substrate was not evaluated.

This is the first study on the performance of TRM vs FRP investigating the debonding mechanism of the retrofitting systems at high temperature. In specific, medium-scale and full-scale T-beams that were strengthened in shear, are tested at both ambient and high temperature under monotonic loading to failure. Parameters studied on medium-scale beams include the matrix used to impregnate the fibres, namely resin or mortar, resulting in two strengthening systems (TRM or FRP), the level of high temperature (100 °C, 150 °C, 250 °C), the strengthening configuration (side-bonding, U-wrapping and full-wrapping), the number of jacketing layers (2 and 3) and the textile properties (geometry, material). The performance of both anchored and non-anchored TRM jacketing in shear strengthening of full-scale T-beams at high temperature was additionally investigated. Details are provided in the following sections.

2. Experimental programme

2.1. Test specimens and investigated parameters

The main objective of this study was to evaluate the effectiveness of TRM versus FRP jacketing in shear strengthening of RC beams subjected to high temperature. The experimental program consists of two Series of tests; Series A and Series B. Series A comprises 28 tests carried out on medium-scale rectangular RC beams, and investigated the following parameters: (a) the matrix used to impregnate the fibres, namely resin or mortar, resulting in two strengthening systems (TRM or FRP), (b) the temperature to which the specimens were exposed (20 °C, 100 °C, 150 °C, 250 °C), (c) the strengthening configuration (side-bonding, U-wrapping and full-wrapping), (d) the number of jacketing layers (2 and 3) and (e) the textile properties (geometry, material). Since the performance of the medium-scale specimens received TRM jacketing at high temperature was very promising, it was decided to assess the TRM system in the shear strengthening of real-scale specimens. Thus, Series B comprises 5 tests performed on full-scale T-beams, investigating: (a) the performance of TRM jacketing in shear strengthening of full-scale T-beams and (b) the use of textile–based anchors as end-anchorage system of the U-jacket, at high temperatures.

2.1.1. Series A: medium-scale rectangular beams

The experimental programme of Series A included 28 tests performed on medium-scale rectangular RC beams simply-supported in asymmetric three-point bending. Sixteen specimens tested at high temperatures (100 °C, 150 °C and 250 °C), whereas the rest twelve specimens tested at ambient temperature.

The total length of the medium-scale rectangular beams was equal to 1677 mm, whereas the effective flexural span was equal to 1077 mm (Fig. 1a), providing adequate anchorage length to the longitudinal reinforcement. To emulate old detailing practices, the beams were designed to be deficient in shear in one of the two shear spans. To achieve this, the critical shorter shear span of

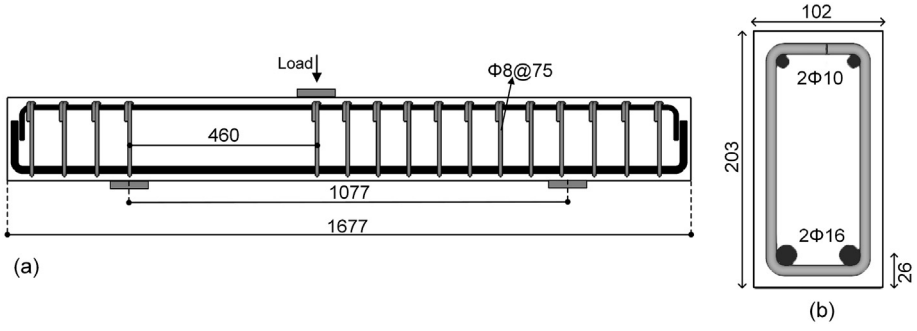

Fig. 1. Medium-scale rectangular beams: (a) Beam geometry and reinforcement; (b) cross section (dimensions in mm).

460 mm length did not include any transverse reinforcement; whereas the larger shear span was over-reinforced including 8-mm diameter stirrups at a spacing of 75 mm. Strengthening was applied only at the critical shear span aiming to increase its shear resistance. By design, the shear force demand in order to develop the full flexural capacity of the (unretrofitted) beams was targeted to be 3 times their shear capacity. As shown in Fig. 1b two 16 mm-diameter and two 10 mm-diameter deformed bars were placed at the tension and compression zone of the rectangular beams, respectively. The geometrical ratio of tensile rebars was 2.2%.

Table 1 presents the details of all specimens of Series A, whereas Fig. 2 illustrates their strengthening configurations. Two beams were tested as-built without receiving strengthening and served as control specimens at ambient (CON_20) and at 150 °C (CON_150). The notation of strengthened specimens is X_YMN_T, where X refers to the strengthening configuration, namely SB for side-bonding, UW for U-wrapping and FW for full-wrapping, Y denotes the matrix material [M for Mortar (TRM system) or R for Resin (FRP system)], M denotes the type of the textile (CL for light carbon, CH for heavy carbon and G for glass), N denotes the number of layers (1, 2, 3 or 7) and T denotes the temperature in which the specimens were exposed during the test (20 °C, 100 °C, 150 °C or 250 °C).

2.1.2. Series B: full-scale T-beams

Five full-scale T-beams were tested in three-point bending. The total length of the T-beams was equal to 6000 mm, whereas the effective flexural span was equal to 3700 mm (Fig. 3a). The T-beams were designed to be deficient in shear in the shorter shear span of 880 mm length that did not include stirrups; whereas the larger shear span was over-reinforced including 10-mm diameter stirrups at a spacing of 100 mm. Strengthening was applied only at the critical shear span aiming to increase its shear resistance. Eight 20 mm-diameter and two 20 mm-diameter deformed bars were placed at the tension and compression zone of the T-beams web, respectively (Fig. 3b) and four 8 mm-diameter deformed bars were additionally placed at the T-beam flanges. The geometrical ratio of tensile steel reinforcement was 3.2%, whereas the effective depth was 385 mm.

Table 1 presents the details of all specimens of Series B, whereas Fig. 4 illustrates the strengthening configurations adopted. One beam was tested as control specimen at ambient temperature (CON), whereas four specimens were strengthened with TRM jackets. The notation of retrofitted specimens is XN_AP_T, where X denotes the type of the textile (CH for heavy carbon), N denotes the number of layers which was 4 for all retrofitted specimens and T denotes the temperature in which the specimens were exposed during the test (20 °C, 150 °C). AP refers to specimens with anchors if any, with A indicating anchors and P denoting the anchorage percentage of the TRM jackets (100%). In specific, specimens CH4_20 and CH4_150 strengthened with 4 U-Wrapped heavy carbon TRM layers and tested at both ambient temperature (20 °C) and at 150 °C, respectively, whereas specimens CH4_A100_20 and

Table 1
Strengthening configuration and material properties of all specimens.

Specimen	Textile used[a]	t[b] (mm)	No. of layers	ρ_f (‰)	Anchorage percentage (%)	Temperature (°C)	Concrete strength (MPa)		Mortar strength (MPa)	
							Compressive strength	Tensile splitting strength	Compressive strength	Flexural strength
CON_20[d]	–	–	–	–	–	20	21.6	2.36	–	–
CON_150	–	–	–	–	–	150	21.8	2.33	–	–
SB_MCH2_20[d]	CH	0.095	2	3.7	–	20	22.6	2.81	28.2	9.21
SB_MCH2_150	CH	0.095	2	3.7	–	150	22.2	1.63	16.2	2.12
SB_MCH3_20[d]	CH	0.095	3	5.6	–	20	22.6	2.81	26.9	8.64
SB_MCH3_150	CH	0.095	3	5.6	–	150	22.2	1.63	16.2	2.12
UW_MCH2_20[d]	CH	0.095	2	3.7	–	20	23.8	2.73	31.1	10.3
UW_MCH2_150	CH	0.095	2	3.7	–	150	22.2	1.63	16.2	2.12
UW_MCH3_20[d]	CH	0.095	3	5.6	–	20	22.6	2.81	26.9	8.64
UW_MCH3_150	CH	0.095	3	5.6	–	150	22.6	1.63	16.2	2.12
UW_MCH3_100	CH	0.095	3	5.6	–	100	20.7	1.64	17.3	2.70
UW_MCH3_250	CH	0.095	3	5.6	–	250	20.7	1.64	17.0	2.55
UW_MCL3_20	CL	0.062	3	3.6	–	20	20.8	2.39	38.7	9.10
UW_MCL3_150	CL	0.062	3	3.6	–	150	20.7	1.64	16.2	2.12
UW_MG7_20	G	0.044	7	6.0	–	20	20.0	1.80	35.5	8.10
UW_MG7_150	G	0.044	7	6.0	–	150	20.7	1.64	16.2	2.12
FW_MCH2_20[d]	CH	0.095	2	3.7	–	20	21.6	2.36	28.2	9.21
FW_MCH2_150	CH	0.095	2	3.7	–	150	21.8	2.33	16.2	2.12
SB_RCH2_20[d]	CH	0.095	2	3.7	–	20	21.6	2.66	–	–
SB_RCH2_150	CH	0.095	2	3.7	–	150	21.8	2.33	–	–
SB_RCH3_150	CH	0.095	3	5.6	–	150	21.8	2.33	–	–
UW_RCH2_20[d]	CH	0.095	2	3.7	–	20	23.8	2.73	–	–
UW_RCH2_150	CH	0.095	3	3.7	–	150	21.8	2.33	–	–
UW_RCH3_20	CH	0.095	3	5.6	–	20	20.8	2.16	–	–
UW_RCH3_150	CH	0.095	3	5.6	–	150	20.8	2.16	–	–
UW_RCH3_100	CH	0.095	3	5.6	–	100	24.6	2.47	–	–
FW_RCH2_20	CH	0.095	1	1.9	–	20	21.6	2.36	–	–
FW_RCH2_150	CH	0.095	2	3.7	–	150	21.8	2.33	–	–
CON[c,e]	–	–	–	–	–	20	14.0	1.39	–	–
CH4_20[c,e]	CH	0.095	4	3.8	–	20	14.0	1.39	36.1	8.12
CH4_150[c]	CH	0.095	4	3.8	–	150	14.5	1.44	22.9	2.83
CH4_A100_20[c,e]	CH	0.095	4	3.8	100	20	13.1	1.23	33.4	8.41
CH4_A100_150[c]	CH	0.095	4	3.8	100	150	13.8	1.25	19.3	2.91

[a] CH: Heavy-weight carbon-fibre textile; CL: Light-weight carbon-fibre textile; G: Glass-fibre textile.
[b] Nominal thickness of textile in one direction based on the equivalent smeared distribution of fibres.
[c] Full-scale T-beams.
[d] Specimens included in Tetta et al., 2015 [23].
[e] Specimens included in Tetta et al., 2016 [26].

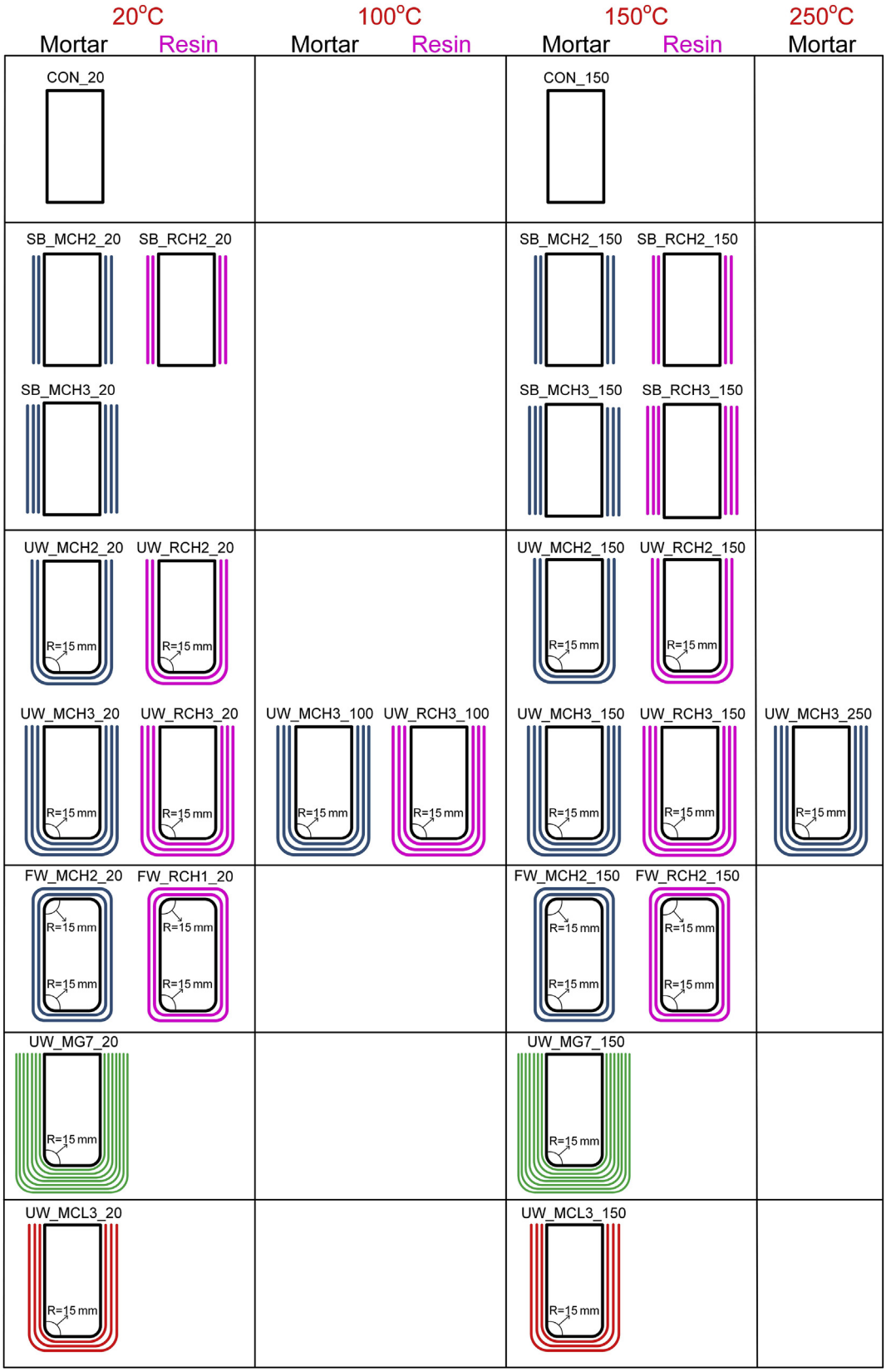

Fig. 2. Schematic representation of different strengthening configurations adopted in medium-scale rectangular beams.

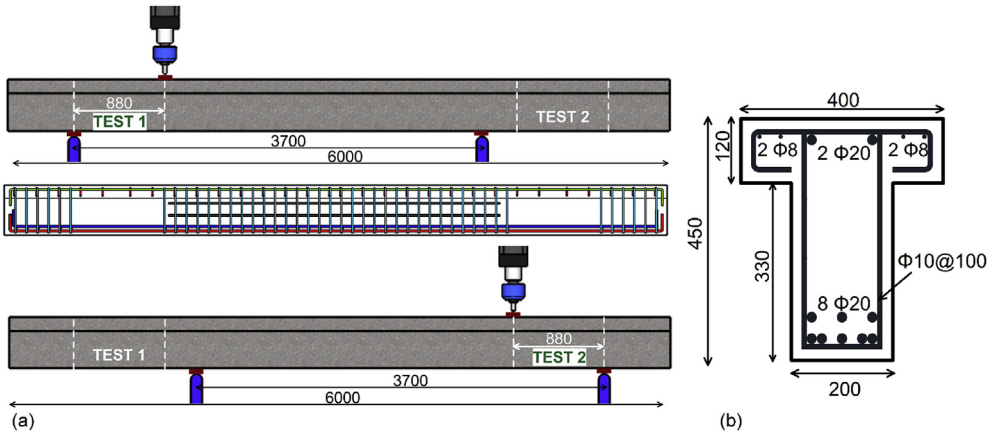

Fig. 3. Full-scale T-beams: (a) Beam geometry and reinforcement; (b) cross section (dimensions in mm).

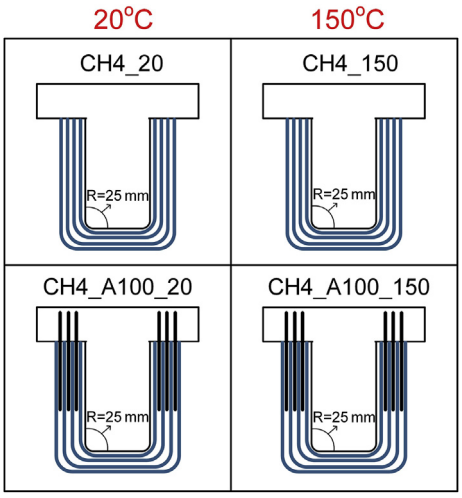

Fig. 4. Schematic representation of different strengthening configurations adopted in full-scale T-beams.

CH4_A100_150 strengthened with 4 U-Wrapped heavy carbon TRM layers anchored by 100% (with fifteen anchors per side) and tested at both ambient temperature (20 °C) and at 150 °C, respectively.

2.2. Materials and strengthening procedure

The medium-scale beams were cast in groups of four using the same concrete mix design. The full-scale T-beam specimens were cast in one batch of ready-mix concrete. The compressive and the tensile splitting strength of concrete were obtained experimentally on the day of testing by conducting standard tests on cylinders of 150 mm-diameters and of 300 mm-height. The results are summarized in Table 1 (average values of 3 cylinders). The 16 and 10 mm-diameter longitudinal bars used in specimens of Series A had a yield stress of 547 MPa and 552 MPa, respectively (average of 3 specimens). The corresponding value for the 8 mm-diameter bars used in both medium-scale and full-scale T-beams was 568 MPa. The 20 and 10 mm-diameter longitudinal bars used in Series B had a yield stress of 571 MPa and 552 MPa, respectively (average of 3 specimens).

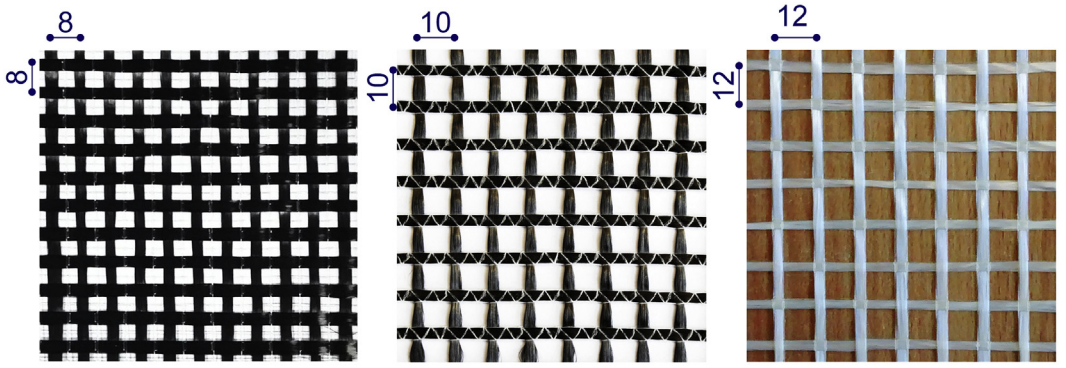

(a)	(b)	(c)
Material: Carbon fibres	Material: Carbon fibres	Material: Glass fibres
Nominal thickness: 0.062 mm	Nominal thickness: 0.095 mm	Nominal thickness: 0.044 mm
Weight: 220 g/m^2	Weight: 348 g/m^2	Weight: 220 g/m^2
E_f : 225 GPa	E_f : 225 GPa	E_f : 74 GPa
f_{fu}: 4800 MPa	f_{fu}: 3800 MPa	f_{fu}: 1400 MPa

Fig. 5. Textiles used in this study: (a) light carbon-fibre textile; (b) heavy carbon-fibre textile; (c) glass-fibre textile (dimensions in mm).

Three different textile reinforcements with equal quantity of fibres in two orthogonal directions were used; two carbon fibre textiles (a light-weight and a heavy-weight one) and a glass fibre textile. The weight of the light carbon textile reinforcement was 220 g/m^2, whereas its nominal thickness (based on the equivalent smeared distribution of fibres) was 0.062 mm (Fig. 5a). The weight of the heavy carbon textile reinforcement was 348 g/m^2, whereas its nominal thickness was 0.095 mm (Fig. 5b). The heavy carbon textile was also used for the fabrication of all the textile-based anchors. Finally, the glass textile was of 220 g/m^2 weight with nominal thickness equal to 0.044 mm (Fig. 5c). The tensile strength (f_{fu}) and the modulus of elasticity (E_f) of the textile reinforcements according to the manufacturer datasheets are included in Fig. 5.

It is noted that seven layers of glass fibre textile are equivalent to one layer of carbon fibre textile in terms of axial stiffness, which is expressed by the product n_ℓ t E_f [(7*0.044*74)/(1*0.095*225) = 1.07], where n_ℓ is the number of TRM layers, t is the nominal thickness of the textile and E_f is the elastic modulus of the fibres. In accordance, two heavy-weight carbon layers are equivalent to three light-weight carbon layers [(2*0.095*225)/(3*0.062*225) = 1.02].

For the TRM jacketed specimens, an inorganic dry binder consisting of cement and polymers at a ratio of 8:1 by weight was used. The water-binder ratio in the mortar was 0.23:1 by weight, resulting in plastic consistency and good workability. Table 1 summarizes the strength properties of the mortar (average values of 3 specimens), which were obtained experimentally on the day of testing using prisms of 40 × 40 × 160 mm dimensions, according to the EN 1015-11 [30]; at various temperature levels (20 °C, 100 °C, 150 °C or 250 °C). For the FRP retrofitted specimen, a commercial epoxy with an elastic modulus of 3.8 GPa and a tensile strength of 30 MPa was used, whereas its T_g is equal to 68 °C (according to the manufacturer datasheets).

Prior to strengthening a thin layer of concrete cover was removed and a grid of groves (2–3 mm deep) was created as shown in Fig. 6a, using a grinding machine. The corners of the medium-scale beams (Series A) receiving UW or FW jackets were rounded to a radius of approximately 15 mm in order to avoid stresses concentration, whereas the corresponding value for the full-scale T-beams (Series B) was 25 mm. For FRP-jacketed specimens the first textile layer was applied on the top of the first resin layer and was then impregnated in-situ with resin using a plastic roll (Fig. 6b). For TRM-jacketed specimens the mortar was applied in approximately 2 mm-thick layers with a smooth metal trowel. After application of the first mortar layer on the (dampened) concrete surface, the textile was applied and pressed slightly into the mortar, which protruded through all the perforations between the fibre rovings. The next mortar layer covered the textile completely, and the operation was repeated until all textile layers were applied (Fig. 6c). Of crucial importance in this method, as in the case of epoxy resins, was the application of each mortar layer while the previous one was still in a fresh state.

The anchorage system of specimens CH4_A100_20 and CH4_A100_150 consists of textile-based anchors [26,31]. The fan-shaped part of the anchors (see Fig. 7a) serves for the distribution of stresses between the textile reinforcement to be anchored and the anchor itself. The dowel part of the anchor (see Fig. 7a) serves for its installation into holes and anchorage into the concrete slab (Fig. 7c). An epoxy resin with tensile strength, modulus of elasticity and T_g equal to 72.4 MPa, 3.2 MPa and 82 °C (according to the manufacturer datasheets), respectively, was used to impregnate the fibers of the anchors and to fill the holes in which the anchors were installed. The geometry of the textile-based anchor is given in Fig. 7b. Fifteen textile-based anchors were applied on each side of T-beam end providing the full anchorage of the four heavy carbon TRM layers; 5 anchors were placed in each of the three interfaces between two consecutive TRM layers (3 × 5 = 15, Fig. 7c). The procedure that was followed to form the anchors, prepare them for use on the day of the strengthening and apply them in T-beams is described in details in Tetta et al. [26].

2.3. Experimental setup and procedure

All beams were subjected to monotonic three-point loading using a stiff steel reaction frame. Vertically positioned, 500 kN-

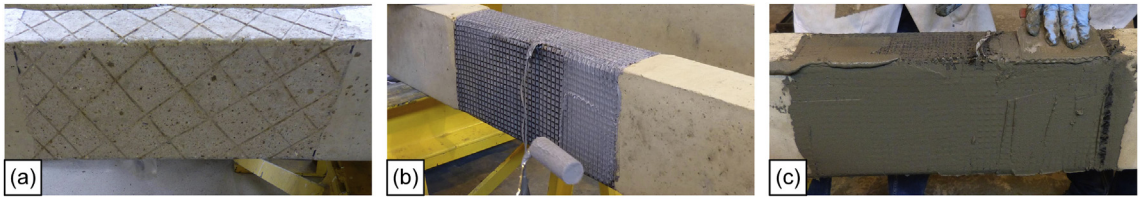

Fig. 6. (a) Prepared concrete surface before strengthening; (b) impregnation of the textile fibres with epoxy resin; (c) application of an extra layer of mortar on the top of the final textile layer.

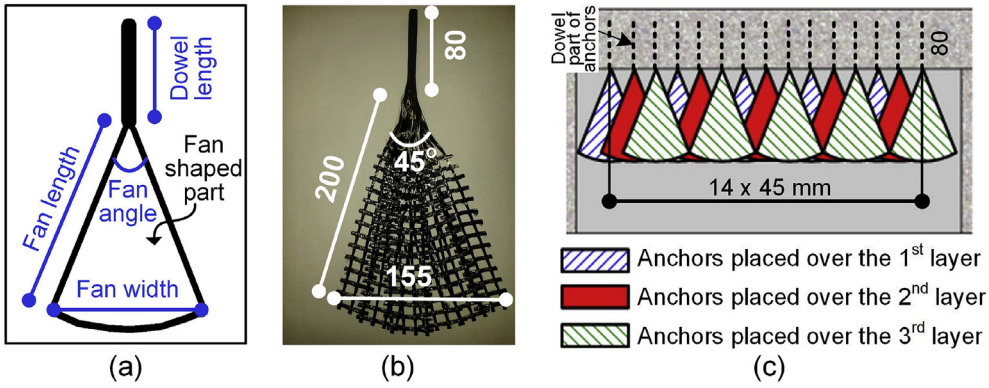

Fig. 7. (a) Sketch of textile-based anchor; (b) geometry of the textile-based anchor; (c) configuration of anchors in specimens CH4_A100 and CH4_A100_150.

capacity and 1000 kN-capacity servo-hydraulic actuators were used for the application of the load on the medium-scale rectangular beams and full-scale T-beams, respectively. The beams tested under high temperature were heated until the target high temperature was reached. After the target high temperature was reached the application of the monotonic loading started. The temperature was kept constant during loading.

The specimens of Series A and B were loaded at displacement rates of 0.02 mm/s and 0.01 mm/s, respectively. As illustrated in Fig. 8a and b, for the specimens of Series A and B respectively, the vertical displacement of the beam was measured at the position of load application using an external LVDT (Linear Variable Differential Transducer); the displacement measured from this sensor was used to plot the load-displacement response curves of the specimens.

The heating system used to provide heating in the critical shear span of medium-scale rectangular beams and full-scale T-beams is depicted in Fig. 9a and Fig. 9b, respectively. The heating system consists of eight 1000 W ceramic heaters of 60 mm height, 245 mm width and 30 mm thickness. The maximum surface temperature of each single heater is 700 °C and has 5000–10000 h working life. Ceramic heaters were placed into steel cases that were fixed at a stainless steel frame, as shown in Fig. 9a and b. Four heaters were placed on each side of the beam at 100 mm distance from the beam surface. As shown in Fig. 9b, a protection steel cage was covering the area subjected to heating in order to prevent a possible touch of the jacket with the heaters after the failure of the specimen.

For specimens tested at high temperatures, ten (type K) thermocouples were affixed to the concrete surface (5 on each side) of the beam before the application of the strengthening system (Fig. 8a and b). Their distribution ensured that the desired temperature was reached along the critical shear span. In specimen CH4_A100_150, two (one on each side) additional thermocouples (A1 and A2) were applied at the end of the dowel part of the central anchor (Fig. 8b); whereas in specimens FW_MCH2_150 and FW_RCH2_150 one additional thermocouple (T3) was applied at the top of the beam (Fig. 8a). The temperature of the beams was controlled by the central thermocouples (C1 and C2, Fig. 8a and b). All data was synchronized and recorded using a fully-computerized data acquisition system. It is noted that the maximum variation from the target temperature recorded on the beams sides was 4–5 °C, indicating the effectiveness of the heating system in developing even heating over the selected zone.

3. Experimental results

3.1. Series A: medium-scale rectangular beams

The response of all medium-scale beams strengthened with heavy carbon textile tested at 150 °C, as well as their counterparts tested at ambient temperature are presented in Fig. 10a–e in the form of load – displacement curves. Fig. 10f and g presents the load – displacement curves for specimens strengthened with light carbon and glass TRM jacketing, respectively. Key results of these specimens are presented in Table 2. They include for both ambient temperature and 150 °C: The peak load; the observed failure mode; the contribution of the jacket to the total shear resistance, V_f, which is calculated as the shear resistance of the strengthened specimen minus the shear resistance of the control specimen, $V_{R,con}$; the shear capacity increase due to strengthening, which is expressed by the ratio, $V_f/V_{R,con}$. The last column presents the reduction of the contribution of the jacket to the total shear resistance due to the effect of high temperature, which is expressed by the ratio, $(V_f^{A.T.}-V_f^{H.T.})/V_f^{A.T.}$. It is worth mentioning that calculation of V_f values have been based on the simplified hypothesis that the two mechanisms of carrying forces (concrete contribution and jacket contribution)

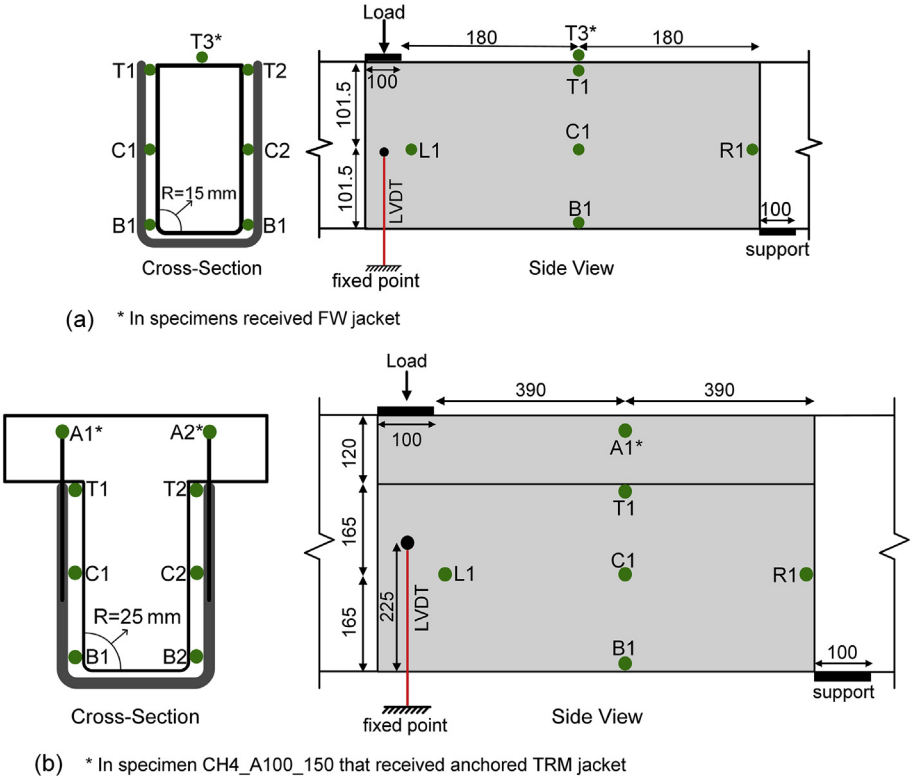

Fig. 8. Configuration of all the thermocouples and the LVDT at the shear-critical span in (a) medium-scale rectangular beams and (b) full-scale T-beams.

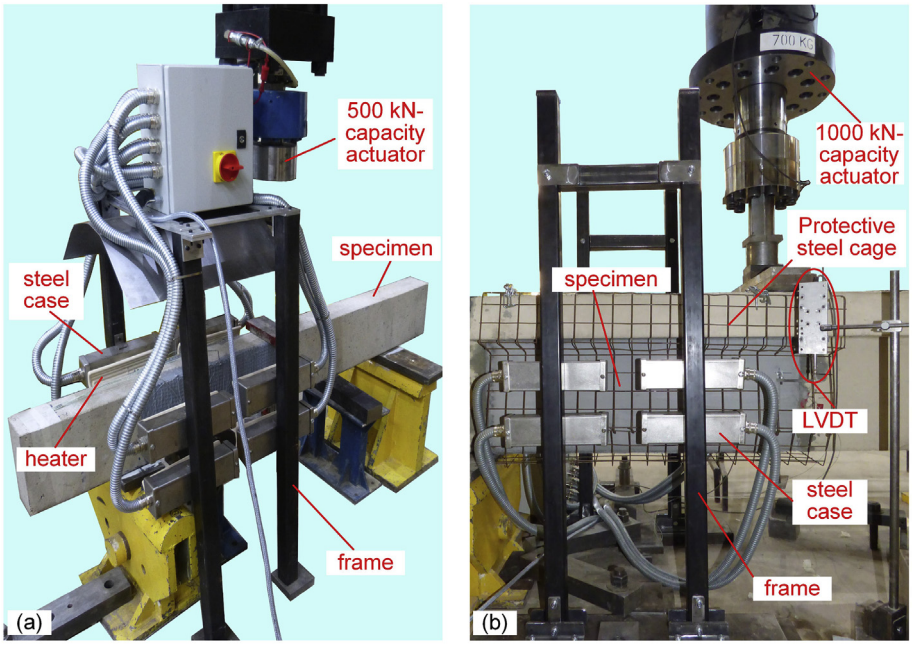

Fig. 9. (a) Test set-up and heating system of medium-scale rectangular beams; (b) Test set-up and heating system of full-scale T-beams.

are superimposed without considering any interaction between them. The interaction between mechanisms of carrying forces is more pronounced when stirrups are used. Thus, other approaches for concrete members strengthened in shear with FRPs, take into account the interaction between the steel and FRP contributions to the shear capacity [32,33].

Fig. 10h and i presents the load – displacement curves of specimens strengthened with three heavy carbon TRM and FRP layers, respectively and tested at different temperatures. In particular, both FRP and TRM-strengthened specimens tested at 100 °C and 150 °C, whereas a TRM specimen was additionally tested at 250 °C. Key results of the aforementioned specimens are also presented in Table 3. A detailed description of the results for control, FRP and TRM specimens at both ambient and high temperature follows.

The control beam at ambient temperature (CON_20) failed in shear at an ultimate load of 52 kN ($V_{R,con}$ = 29.7 kN) after the formation of a large shear crack in the critical span. The control beam tested at 150 °C (CON_150) failed in shear in identical manner with specimen CON_20, namely at the same ultimate load and by forming a large shear crack in the critical shear span (Fig. 11a). Thus, the response and failure mode of the un-retrofitted RC beam was not affected by its exposure to 150 °C.

All beams strengthened with SB or UW FRP jackets and tested at ambient temperature failed in shear at an ultimate load substantially higher than that of the control beam. The peak load attained by specimens SB_RCH2_20, UW_RCH2_20 and UW_RCH3_20 was 125, 126 and 139 kN, respectively, yielding 141%, 145% and 168% increase in the shear capacity. In all these specimens failure occurred due to FRP debonding, including peeling off of the concrete cover (i.e. Fig 11b). Specimen FW_RCH2_20 reached its ultimate moment capacity at a load of 152 kN and failed due to concrete crushing after yielding of the tensile longitudinal reinforcement.

All beams strengthened with SB or UW FRP jacketing and tested at 150 °C failed in shear at ultimate loads dramatically lower than their counterparts tested at 20 °C. The peak load attained by specimens SB_RCH2_150, SB_RCH3_150, UW_RCH2_150 and UW_RCH3_150 was 51, 51, 62 and 62 kN (Fig. 10a–d), respectively, resulting in 0%, 0%, 20% and 20% increase in the shear capacity. Thus, the contribution of the FRP jacket to the total shear resistance of the beam at 150 °C decreased by 100%, 100%, 86% and 88%, respectively. In all these specimens, adhesive failures at the concrete-resin interface were observed (Fig. 11c–f). In specific, FRP jackets delaminated at the concrete-resin interface without peeling off of the concrete cover due to the poor bond behaviour of epoxy resin at temperature above the T_g. Finally, the fully wrapped specimen FW_RCH2_150 reached an ultimate load of 129 kN, which yields at least 22.8% decrease in the effectiveness of the FRP jacket. Failure of this specimen was due to slippage of the vertical fibre rovings (Fig. 11g) through the resin (which was completely decomposed due to high temperature) combined with delamination of the last textile layer used for overlapping at the top of the beam (Fig. 11h). The temperature recorded from the thermocouple placed at the top of the beam (T3, see Fig. 8a) at the instant of failure was 138 °C.

Specimen UW_RCH3_100 reached a higher load (86 kN) with respect to specimen UW_RCH3_150 (62 kN) resulting in 67% increase in the shear capacity compared to the control specimen. The effectiveness of the FRP jacket decreased by 60% due to its exposure at 100 °C. Adhesion failure at the resin-concrete interface was also observed in specimen UW_RCH3_100 (Fig. 11i) as was the case for specimen UW_RCH3_150 (Fig. 11e–f).

TRM jacketed specimens SB_MCH2_20, SB_MCH3_20, UW_MCH2_20, UW_MCH3_20, UW_MCL3_20 and UW_MG7_20, tested at ambient temperature, failed in shear at an ultimate load of 89, 109, 120, 131, 118 and 144 kN, respectively, resulting in 71%, 111%, 131%, 152%, 128% and 178% increase in the shear capacity. Failure in specimens SB_MCH2_20, SB_MCH3_20 and UW_MCH2_20 was attributed to debonding of the TRM jacket at a large part (approximately 2/3) of the shear span which was accompanied by peeling off of the concrete cover (Fig. 11j). Specimens UW_MCH3_20, UW_MCL3_20 and UW_MG7_20 failed in shear due to debonding of the U-jacket at the full-length of the shear span (Fig. 11k). Finally, specimen FW_MCH2_20 reached its ultimate moment capacity and (identically to FW_RCH2_20) failed in flexure

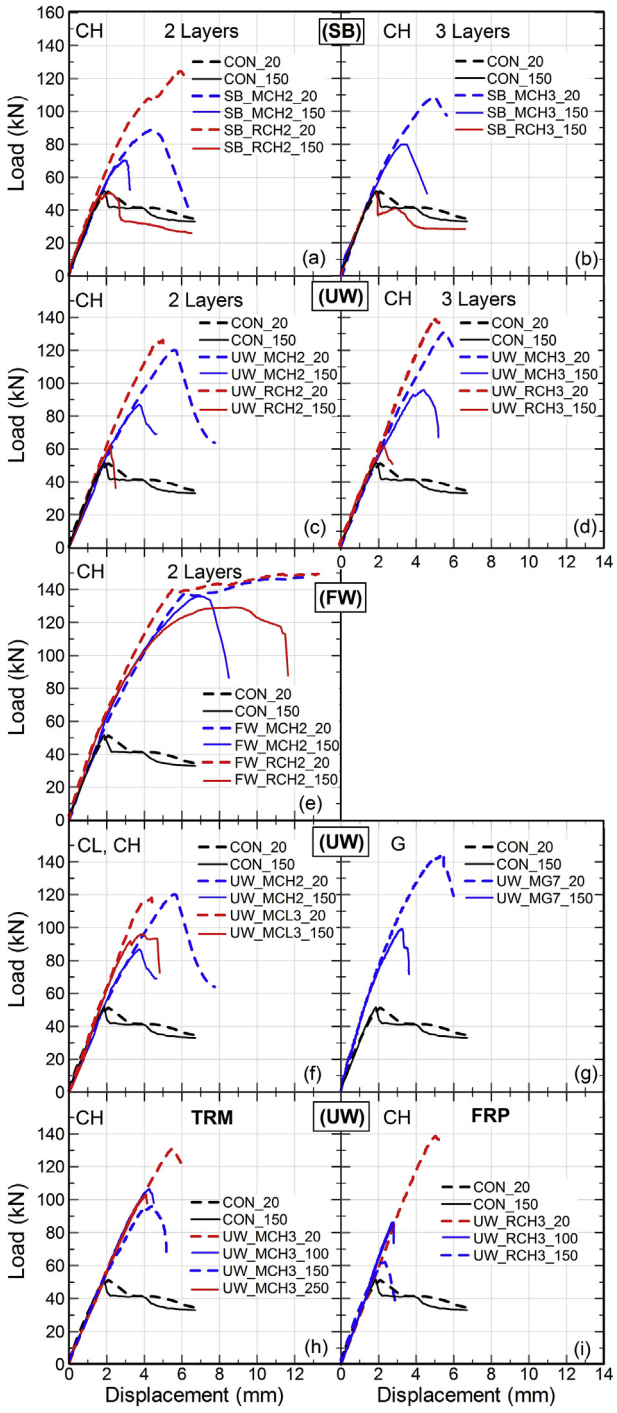

Fig. 10. Load versus vertical displacement curves for all medium-scale rectangular beams.

due to concrete crushing at the compression zone.

The behaviour of the TRM jacketed specimens at 150 °C was far better compared with their FRP counterparts. Specimens SB_MCH2_150, UW_MCH2_150, FW_MCH2_150, SB_MCH3_150, UW_MCH3_150, UW_MCL3_150 and UW_MG7_150, reached an ultimate load of 70, 87, 136, 81, 96, 96 and 99 kN, respectively, resulting in 37%, 67%, 162%, 57%, 84%, 84%, 91% increase of the shear capacity. The effectiveness of the TRM jacketing at 150 °C was decreased by 47.6%, 48.7%, 17.2%, 48.5%, 44.4%, 34.2% and 49.1%, respectively. The failure of specimens SB_MCH2_150, UW_MCH2_150 and FW_MCH2_150 strengthened with two layers of TRM jackets was associated with damage of the TRM jackets that included the following local phenomena: (a) slippage of the vertical fibre rovings through the mortar, and (b) partial rupture of the fibres crossing the shear crack (Fig. 11l–m). Finally, specimens SB_MCH3_150, UW_MCH3_150, UW_MCL3_150 and UW_MG7_150, which strengthened with 3 layers of carbon fibre or 7 of glass fibre textile, failed due to debonding of the TRM jacket from the concrete substrate with peeling off of the concrete cover (Fig. 11n–q), demonstrating good bond between the concrete substrate and the TRM jacket at high temperature.

The peak load attained by specimens UW_MCH3_100 and UW_MCH3_250, at 100 °C and 250 °C, respectively, was 107 kN and 103 kN, yielding 104% and 98% increase in the shear capacity. The contribution of the jacket to the total shear resistance of the beam decreased by 31% and 36%, respectively compared to the corresponding specimen tested at ambient temperature. Failure of these specimens was due to debonding of the jacket from the concrete substrate with peeling off of the concrete cover (i.e. Fig. 11r) identically to specimen UW_MCH3_150 (Fig. 11o).

3.2. Series B: full-scale T-beams

The load-displacement curves of the full-scale specimens are presented in Fig. 12. Key results are also presented in Table 2. The control beam (CON) tested at ambient temperature failed in shear at an ultimate load of 163 kN ($V_{R,con}$ = 124 kN). A large shear crack was firstly formed in the web of the critical shear span (Fig. 13a), which was then propagated into the flange of the T-beam and resulted in significant load drop. It was decided to not test a control beam at 150 °C, as based on the test results of Series A, the response of the un-retrofitted RC beam was not affected at this temperature.

The two TRM strengthened specimens tested at ambient temperature failed in shear and displayed considerably higher shear resistance compared to the control specimen. In particular, specimen CH4_20 reached an ultimate load of 288 kN, resulting in 77% increase in the shear capacity compared to the control specimen. Its failure was due to debonding of the TRM jacket at a large part (approximately 2/3) of the shear span (Fig. 13b), which was also accompanied by peeling off of the concrete cover. Specimen CH4_A100_20 that had anchors (see Fig. 7) failed in shear at an ultimate load of 473 kN, yielding 190% increase in the shear capacity, with respect to the control specimen. Failure of specimen CH4_A100_20 was attributed to anchors pull-out (8 on each side) due to concrete splitting at the two flanges (Fig. 13c).

The two TRM jacketed specimens tested at 150 °C failed in shear displaying considerably higher shear resistance compared to the control specimen but lower shear resistance with respect to the corresponding specimens tested at ambient temperature. Specimens CH4_150 and CH4_A100_150 reached an ultimate load of 249 kN and 319 kN, resulting in 53% and 96%, respectively increase in the shear capacity. The effectiveness of the TRM jacketing decreased by 30.5% and 49.6%, respectively, compared to the corresponding specimens tested at ambient temperature. The failure of specimen CH4_150 was due to debonding of the TRM jacket from the concrete substrate (Fig. 13d) including peeling off of the concrete cover (Fig. 13e). Finally, the failure of specimen CH4_A100_150 was attributed to debonding of the jacket including peeling off of the concrete cover due to failure of anchors (Fig. 13f). In particular, all anchors were pulled-out due to the softening and decomposition of the epoxy resin used to fill the holes into which the dowel part of anchors was anchored, as the mean temperature at the top of central anchors (as this was recorded from the thermocouples A1 and A2, Fig. 8b) was 128 °C, namely well above from the T_g (82 °C) of the epoxy resin.

Table 2
Summary of test results of beams tested at ambient temperature and at 150 °C.

Specimen	Ambient temperature (20 °C)				High temperature (150 °C)				$(V_f^{A.T}-V_f^{H.T})/V_f^{H.T}$ (%)
	Peak load (kN) ((kN)	Failure mode	V_f (kN)	$V_f/V_{R,con}$ (%)	Peak load (kN)	Failure mode	V_f (kN)	$V_f/V_{R,con}$ (%)	
CON	52	shear[a]	–	–	52	shear[a]	–	–	–
SB_MCH2	89	shear[c]	21	71	70	shear[b]	11	37	47.6
SB_MCH3	109	shear[c]	33	111	81	shear[c]	17	57	48.5
UW_MCH2	120	shear[c]	39	131	87	shear[b]	20	67	48.7
UW_MCH3	131	shear[c]	45	152	96	shear[c]	25	84	44.4
UW_MCL3	118	shear[c]	38	128	96	shear[c]	25	84	34.2
UW_MG7	144	shear[c]	53	178	99	shear[c]	27	91	49.1
FW_MCH2	153	flexural	58[h]	195	136	shear[b]	48	162	17.2
SB_RCH2	125	shear[c]	42	141	51	shear[d]	0	0	100.0
SB_RCH3	–	shear[c]	–	–	51	shear[d]	0	0	100.0
UW_RCH2	126	shear[c]	43	145	62	shear[d]	6	20	86.0
UW_RCH3	139	shear[c]	50	168	62	shear[d]	6	20	88.0
FW_RCH2	152	flexural	57[h]	192	129	shear[e]	44	148	22.8
CON[i]	163	shear[a]	–	–	–	–	–	–	–
CH4[i]	288	shear[c]	95	77	249	shear[c]	66	53	30.5
CH4_A100[i]	473	shear[f]	236	190	319	shear[g]	119	96	49.6

[a] Tensile diagonal cracking.
[b] Slippage of the vertical fibre rovings through the mortar and partial fibres rupture.
[c] Debonding of the jacket with peeling off of the concrete cover.
[d] Adhesive failure at the resin-concrete interface.
[e] Slippage of the vertical fibre rovings through the epoxy resin and delamination of the textile used for overlapping.
[f] Pull-out of anchors due to concrete splitting in the slab.
[g] Pull-out of all anchors due to adhesive bond failure.
[h] This value can be considered as a lower limit of V_f due to the flexural failure.
[i] Full-scale T-beams.

Table 3
Summary of tests results of medium-scale beams tested at ambient temperature, 100 °C, 150 °C and 250 °C.

	Specimen	UW_MCH3	UW_RCH3
Ambient temperature (20 °C)	Peak Load (kN)	131	139
	Failure mode	Shear[a]	Shear[a]
	V_f (kN)	45	50
	$V_f/V_{R,con}$ (%)	152	168
Elevated temperature 1 (100 °C)	Peak Load (kN)	107	86
	Failure mode	Shear[a]	Shear[b]
	V_f (kN)	31	20
	$V_f/V_{R,con}$ (%)	104	67
	$(V_f^{A.T}-V_f^{H.T.})/V_f^{A.T.}$ (%)	31	60
Elevated temperature 2 (150 °C)	Peak Load (kN)	96	62
	Failure mode	Shear[a]	Shear[b]
	V_f (kN)	25	6
	$V_f/V_{R,con}$ (%)	84	20
	$(V_f^{A.T}-V_f^{H.T.})/V_f^{A.T.}$ (%)	44	88
Elevated temperature 3 (250 °C)	Peak Load (kN)	103	–
	Failure mode	Shear[a]	–
	V_f (kN)	29	–
	$V_f/V_{R,con}$ (%)	98	–
	$(V_f^{A.T}-V_f^{H.T.})/V_f^{A.T.}$ (%)	36	–

[a] Debonding of the jacket with peeling off of the concrete cover.
[b] Adhesive failure at the resin-concrete interface.

4. Discussion

4.1. Effect of investigated parameters for medium-scale beams tested at high temperature

All specimens tested at high temperature failed in shear, allowing for the evaluation of the effectiveness of all strengthening systems. In terms of the various parameters investigated in this experimental programme, an examination of the results in terms of shear capacity and failure modes, revealed the following information.

4.1.1. Matrix material (TRM vs. FRP jackets)

The matrix material (mortar vs epoxy resin) significantly affects the response of the strengthened beams at high temperature. In the following paragraphs, the effect of the adhesive material on the performance of jacketed specimens exposed to high temperature is studied, as the strengthening configuration (4.1.1.1), the number of layers (4.1.1.2) and the temperature to which the specimens are exposed (4.1.1.3) vary.

4.1.1.1. Strengthening configuration. The curves in Fig. 14a illustrate the effect of the strengthening configuration (SB, UW or FW) on the shear capacity enhancement (V_f/V_{con} ×100%) at 150 °C. In FRP-strengthened specimens, the shear capacity was only increased by 6 kN (20%) when UW jackets were applied instead of SB ones for both 2 and 3 layers. On the other hand in TRM-strengthened specimens, the effectiveness of the UW jackets (expressed as the

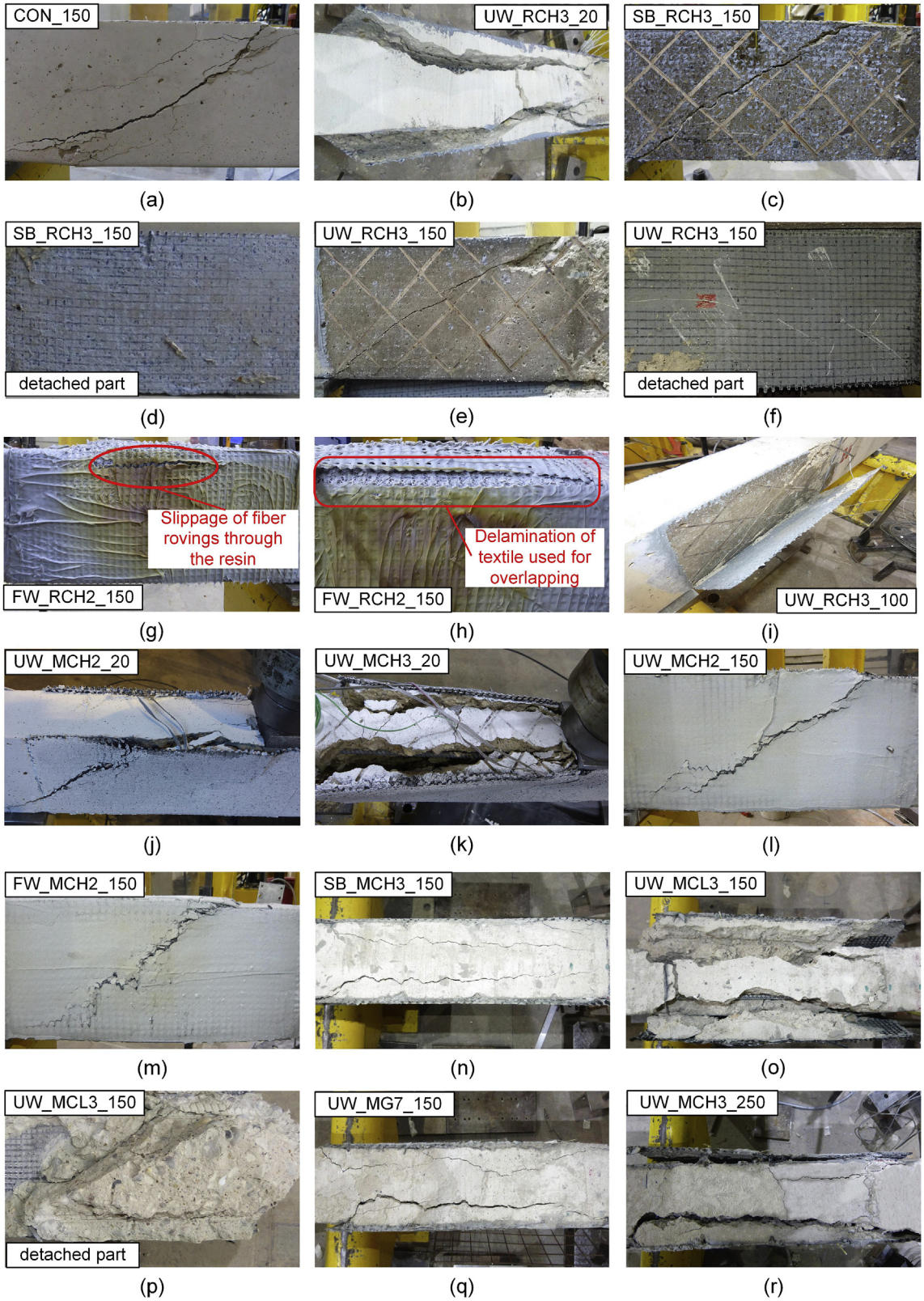

Fig. 11. Failure modes of medium-scale rectangular beams: (a) CON_150 – dominant shear crack in specimen; (b) specimens UW_RCH3_20 – debonding of the jacket: peeling off of the concrete cover; (c)-(f) specimens SB_RCH3_150 and UW_RCH3_150 – adhesive failure at the resin-concrete interface; (g) specimen FW_RCH2_150 – slippage of the vertical fibre rovings through the epoxy resin; (h) specimen FW_RCH2_150 – delamination of textile used for overlapping; (i) specimen UW_RCH3_100 – adhesive failure at the resin-concrete interface; (j)-(k) specimens UW_MCH2_20 and UW_MCH3_20 – debonding of the jacket: peeling off of the concrete cover; (l)-(m) specimens UW_MCH2_150 and FW_MCH2_150 – local damage of the jacket; (n)-(r) specimens SB_MCH3_150, UW_MCL3_150, UW_MG7_150 and UW_MCH3_250 – debonding of the jacket: peeling off of the concrete cover.

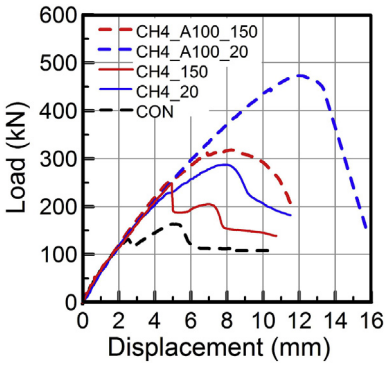

Fig. 12. Load versus vertical displacement curves for full-scale T-beams.

shear capacity enhancement) was 1.81 and 1.47 times the effectiveness of the SB jackets for 2 and 3 layers, respectively. FW jacketing was the most effective configuration for both strengthening systems. In particular, the effectiveness of the FW jacket was 2.4 and 7.3 times the UW jacket effectiveness in case of two TRM and FRP layers, respectively. The effect of SB and UW configurations on the shear capacity enhancement at high temperature was quite similar to this observed at ambient temperature for both TRM and FRP systems, whereas the benefit of applying FW was more pronounced at high temperature than ambient temperature for both strengthening systems (TRM, FRP).

4.1.1.2. Number of layers. The effect of the number of layers on the shear capacity enhancement for SB and UW strengthening

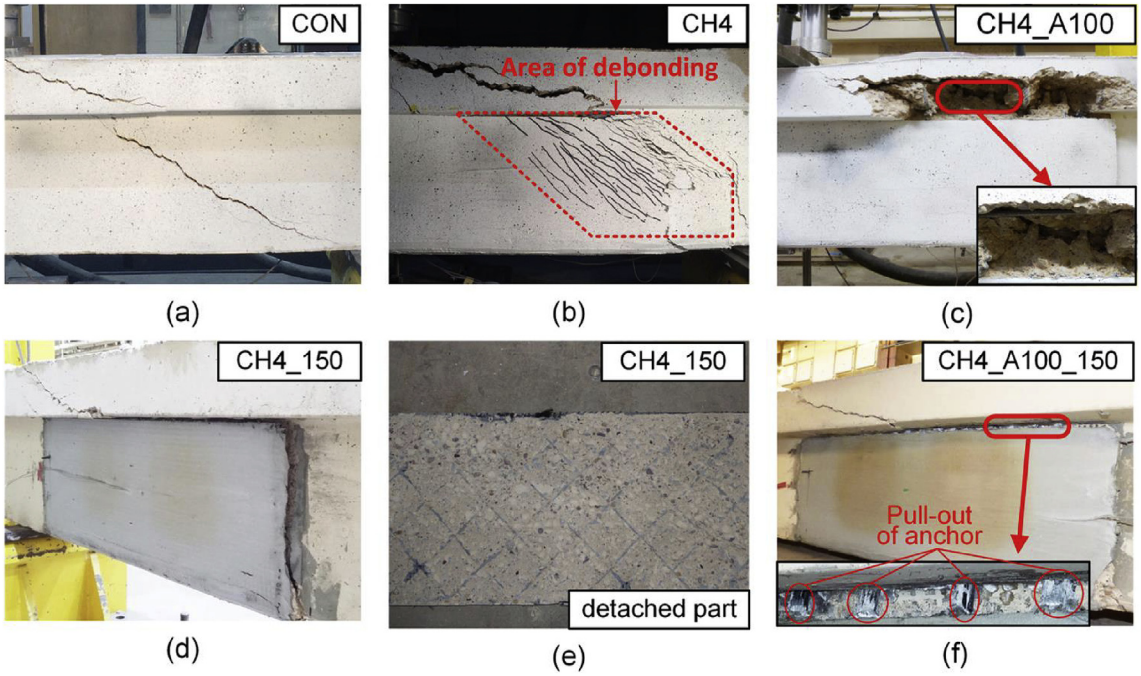

Fig. 13. Failure modes of full-scale T-beams: (a) Dominant shear crack in the control beam; (b) specimen CH4 – debonding of the TRM jacket: peeling off of the concrete cover; (c) failure of specimen CH4_A100 due to concrete splitting in the slab; (d) debonding of the TRM jacket in specimen CH4_150: peeling off of the concrete cover; (e) specimen CH4_150 – detached part of TRM jacket including concrete cover; (f) specimen CH4_A100_150 – pull-out of all anchors due to bond adhesive failure.

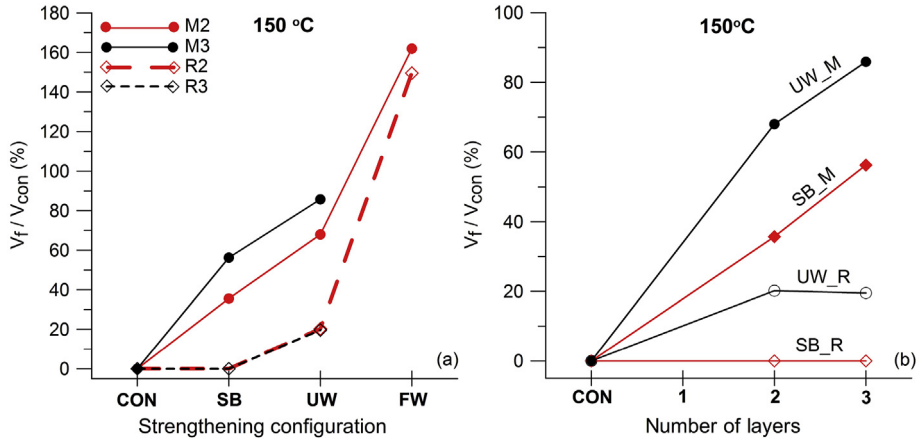

Fig. 14. (a) Effect of strengthening configuration on the shear capacity enhancement at high temperature; (b) effect of number of layers on the shear capacity enhancement at high temperature.

configurations under high temperature conditions is illustrated in Fig. 14b. Increasing the amount of reinforcement from 2 to 3 layers, resulted in 1.55 and 1.25 higher V_f for the beams received SB and UW TRM jackets, respectively. Zero increase in the shear capacity was observed when resin was used as binder for both SB and UW jackets.

When the number of layers was increased from two to three, a change in the failure mode was witnessed in TRM-strengthened specimens tested at high temperature. In particular, the beams received 2 layers of SB and UW TRM jackets failed due to local damage (the vertical fibre rovings crossing the developed shear crack at the jacket experienced a combination of slippage through the mortar and partial rupture Fig. 11l–m). Contrary, the failure mode of specimens received three SB and UW layers is associated to debonding of the jacket from the concrete substrate. Thus, the increase in the number of layers prevented these local phenomena and as a result the damage was shifted to the concrete substrate. This is attributed to the better mechanical interlock conditions created by the overlapping of multiple textile layers as also reported in Refs. [8,23 and 26]. The failure mode of SB and UW FRP-strengthened specimens tested at high temperature was not affected from the increase in the number of layers.

It worth's mentioning that in case of the TRM system, this change in failure mode (from local damage of the TRM jacket to its debonding), witnessed here in specimens with 2 and 3 layers tested at high temperature, was also observed for an increase from 1 to 2 layers in specimens tested at ambient temperature, as reported by Tetta et al. [23]. Local damage of the jacket is observed in case of poor mechanical interlock which is affected from the textile geometry [26], the number of layers [8,23] and the mortar strength. In specimens received 1 TRM layer and tested at ambient temperature, the textile geometry, namely the sparse-mesh pattern of the heavy-carbon textile, mainly caused the slippage of the vertical rovings through the mortar which was although prevented when at least two TRM layers were applied [23].

For specimens received two SB or UW TRM layers and tested at high temperature, the decrease of the mortar strength at high temperature caused damage in the TRM jacket and impaired the mechanical interlock effect activated in Ref. [23] for two TRM layers. At high temperature, the mechanical interlock beneficial effect reappeared when specimens received three SB or UW TRM layers.

4.1.1.3. Temperature. The effect of high temperature on the shear capacity enhancement for specimens received 3 UW layers is depicted in Fig. 15a. The effectiveness of the FRP strengthening system was dramatically reduced from the temperature increase. In specific, the contribution of the FRP jacket to the shear resistance decreased by 60% and 88% when the temperature increased from 20 °C to 100 °C and 150 °C, respectively. The failure mode of both specimens tested at high temperature (UW_RCH3_100 and UW_RCH3_150) was attributed to adhesive failure at the interface between the FRP jacket and the concrete substrate. Thus, the bond between the FRP jacket and the concrete substrate at 100 °C was better than this experienced at 150 °C (as this reflected at the shear capacity increase) but not good enough to shift the failure from the interface (between the jacket and the concrete) to the concrete substrate, as occurred at the corresponding specimen tested at ambient temperature.

The effectiveness of specimens strengthened with 3 TRM layers and tested at 100 °C, 150 °C and 250 °C decreased by 31%, 44% and 36%, respectively. It is striking to note that by increasing the temperature from 150 °C to 250 °C, the contribution of TRM jacket to the shear resistance increased by 16% (Fig. 15a). This could be attributed to flexural and compressive strength of mortar, which as shown in Fig. 15b, at this temperature range, follows a quite similar trend with this of shear capacity enhancement (V_f/V_{con}). Finally, the exposure of TRM-strengthened specimens at different high temperature levels (100 °C, 150 °C and 250 °C) had no effect on the failure mode that was debonding of the jacket from the concrete substrate.

4.1.2. Textile properties (geometry, material)

Specimens UW_MCH2 and UW_MCL3 received correspondingly 2 and 3 layers carbon textile of different geometry, having although the same amount of external reinforcement ($\rho_f = 1.9‰$). The light carbon textile used in specimen UW_MCL3 has denser mesh-pattern than the heavy carbon textile (Fig. 5). The shear capacity increase of both specimens tested at ambient temperature was almost the same and their failure was due to debonding of the TRM jacket from the concrete substrate.

A comparison of the results for specimens UW_MCH2_150 and UW_MCL3_150 shows that the textile geometry can affect the failure mode of specimens exposed to high temperature. In specific, UW_MCH2_150 specimen failed due to local damage of the TRM jacket (Fig. 11l) in contrary to specimen UW_MCL3_150 that failed due to debonding of the TRM jacket from the concrete substrate (Fig. 11o). The difference in failure mode is possibly associated with the dense mesh-pattern of the light-carbon textile used in specimen UW_MCL3_150, which resulted in better fibres distribution along the shear span and therefore the mechanical interlock between the textile and the mortar was improved. Thus, the local damage of the jacket was prevented in specimen UW_MCL3_150

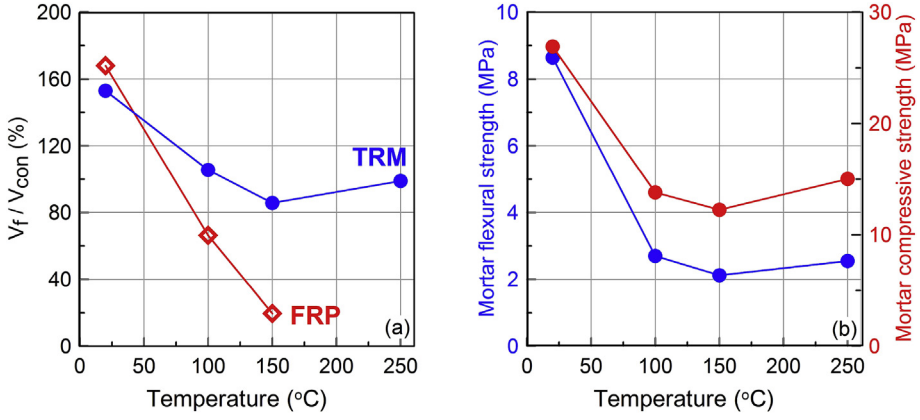

Fig. 15. (a) Effect of temperature on the shear capacity enhancement for both TRM and FRP system; (b) effect of temperature on the mortar flexural strength.

thanks to the better mechanical interlock conditions despite the decreased (due to the high temperature) mortar strength. The shear capacity increase of specimens UW_MCH2_150 and UW_MCL3_150 was 67% and 84%, respectively compared to the control specimen.

Specimen UW_MG7 strengthened with seven glass textile layers had higher shear capacity than specimen UW_MCH3 that received three heavy carbon textile layers, at both ambient and high temperature, despite the fact that seven glass textile layers are equivalent to just one heavy-carbon textile layer (in terms of axial stiffness as explained in Section 2.2). In specific, the shear capacity increase of specimens UW_MG7_20 and UW_MCH3_20 tested at ambient temperature was 178% and 152%, respectively. The corresponding values for specimens tested at 150 °C was 91% and 84%, respectively. All specimens exhibited similar failure mode at both ambient and high temperature, namely debonding of the TRM jacket from the concrete substrate.

4.2. Performance of full-scale T-beams strengthened with TRM jackets at 150 °C

The effectiveness of TRM jacketing in shear strengthening of full-scale beams remained high at 150 °C. In particular, in specimen CH4_150 tested at 150 °C, four heavy carbon TRM layers increased the shear capacity of the beam by 53% compared to the control specimen. The contribution of the TRM jacket to the shear resistance decreased by 30.5% compared to the corresponding specimen tested at ambient temperature. In specimen CH4_A100_150 tested at 150 °C, the full anchorage of four heavy carbon layers provided by 15 anchors per beam's side (see Fig. 7c) improved the effectiveness of the TRM jacket by 80.3% compared with its counterpart specimen without anchors (CH4_150), resulting in 119% increase in the shear resistance compared to the control specimen. The exposure of specimen at 150 °C (CH4_A100_150) resulted in 49.6% decrease in the effectiveness of the anchored TRM jacket.

The T-beam ends received non-anchored jackets (CH4_20, CH4_150) exhibited identical failure mode, namely debonding of the TRM jacket from the concrete substrate, at both ambient temperature and 150 °C. In specimens received anchored TRM jacket, anchors were pulled-out from the slab at both ambient temperature and at 150 °C due to concrete splitting in the slab (CH4_A100_20) and melting of the resin in the anchorage holes (CH4_A100_150), respectively.

5. Stress reduction factor for TRM and FRP systems

For calculating the FRP contribution to the shear capacity of RC members most of the design models use the effective stress of the FRP (σ_{eff}), which can ideally be described as the average stress of the fibres crossing the shear crack. The effective stress of the jacket, σ_{eff} is calculated using Eq. (1) [4]. The experimental values of V_f were calculated according to the approach that the concrete and jacket contribution are superimposed.

$$\sigma_{eff} = V_f \Big/ \left(\rho_f b_w 0.9d\right) \tag{1}$$

For T-beam specimens, the term $0.9d$ in Eq. (1) is replaced from the term d-h_s, where d is the effective depth of the section and h_s the depth of the slab.

The effective stress of FRP or TRM jackets at high temperature, $\sigma_{eff,\ high}$, is a reduced value of their effective stress, σ_{eff}, at ambient temperature. It is expressed by the following equation:

$$\sigma_{eff,high} = k\sigma_{eff} \tag{2}$$

where k is the stress reduction factor with values less than 1.0.

The values of the effective stress of TRM and FRP jackets at both ambient and high temperature, σ_{eff} and $\sigma_{eff,\ high}$, respectively are given in Table 4. In addition, Table 4 includes the stress reduction factor, k. In this study, k value varies with the strengthening system (TRM, FRP), the strengthening configuration (SB, UW and FW) and the level of high temperature (100 °C, 150 °C or 250 °C). In particular, for TRM jackets, k varies from 0.50, which corresponds to four fully anchored TRM layers (applied to full-scale T-beam) exposed to 150 °C to 0.83 which corresponds to two layers of FW jacket exposed at 150 °C. In case of FRP jackets, k significantly varies from 0 and 0.14 for both two and three layers of SB and UW jackets,

Table 4
Experimental values of effective stress and stress reduction factors for TRM and FRP jackets.

		σ_{eff} (MPa)	$\sigma_{eff,high}$ (MPa)	k
		Ambient temperature	150 °C	
TRM	SB_MCH2	347	182	0.52
	SB_MCH3	363	187	0.52
	UW_MCH2	644	330	0.51
	UW_MCH3	496	275	0.56
	UW_MCL3	641	422	0.66
	UW_MG7	489	540	0.51
	CH4	477	328	0.69
	CH4_A100	1177	591	0.50
		Ambient Temperature	**100 °C**	
	UW_MCH3	496	341	0.69
		Ambient Temperature	**250 °C**	
	UW_MCH3	496	319	0.64
		Ambient Temperature	**150 °C**	
	FW_MCH2[a]	958	793	0.83
FRP	SB_RCH2	694	0	0.00
	SB_RCH3	–	0	0.00
	UW_RCH2	710	99	0.14
	UW_RCH3	551	66	0.12
		Ambient Temperature	**100 °C**	
	UW_RCH3	551	220	0.40
		Ambient Temperature	**150°C**	
	FW_RCH2[b]	942	727	0.77

[a] The temperature at the top of the beam was 136 °C at the instant of the peak load.
[b] The temperature at the top of the beam was 138 °C at the instant of the peak load.

respectively tested at 150 °C to 0.77 which corresponds to two FW layers tested at 150 °C. Hence, TRM jackets are more effective than FRP jackets at high temperature, but the effectiveness is sensitive to parameters such as the strengthening configuration and the level of high temperature.

Based on the results of this study, the use of SB or UW FRP jackets is not recommended for shear strengthening of RC beams when fire or high temperature is a critical issue in the design, unless protective (thermal insulation) systems are provided. The fully-wrapped FRP jacket remained quite effective at high temperature. However, the use of closed jackets is not feasible in beams of typical RC buildings or bridge girders due to the presence of concrete slabs or decks, respectively.

SB and UW (both non-anchored and anchored) TRM jackets are applicable for shear strengthening of RC beams exposed to high temperature. Based on the limited experimental data of the present study and before more experimental data will be available, a value of k equal to 0.4 could be used for design beams strengthened in shear with TRM jacketing in case of their exposure to high temperature (up to 250 °C).

6. Conclusions

This paper presents a large experimental investigation on the effectiveness of TRM jackets in shear strengthening of both medium-scale rectangular RC beams and full-scale RC T-beams at high temperature. The main investigated parameters studied on medium-scale rectangular beams include: (a) the strengthening system (TRM or FRP), (b) the level of high temperature to which the specimens are exposed (20 °C, 100 °C, 150 °C, 250 °C), (c) the strengthening configuration (side-bonding, U-wrapping and full-wrapping), (d) the number of jacketing layers (2 and 3) and (e) the textile properties (geometry, material), whereas the effectiveness of both non-anchored and anchored TRM jackets in shear strengthening of full-scale T-beams at high temperature was also studied. The main conclusions drawn from this study are summarized as follows:

- TRM is much more effective in increasing the shear capacity of RC beams subjected to high temperature than FRP jacketing.
- The strengthening configuration affects considerably the shear capacity increase for both TRM and FRP jackets at high temperature. In specific, fully-wrapping (FW) is the most effective strengthening configuration, following by U-wrapping (UW), whereas side-bonding (SB) is the less effective strengthening configuration, for both TRM and FRP jackets.
- The failure mode of SB and UW TRM jacketed specimens tested at high temperature is altered for different number of layers. Increasing them from 2 to 3, prevented the local damage of the TRM jacket and shifted it to the concrete surface. On the other hand, the increase in number of layers has no effect on the shear capacity increase nor the failure mode of SB and UW FRP jackets.
- The exposure of specimens strengthened with 3 layers of TRM or FRP to high temperatures (100 °C, 150 °C, 250 °C) had no effect on their failure mode. The effectiveness of FRP jackets dropped dramatically by increasing the temperature from 100 °C to 150 °C. On the other hand, the effectiveness of TRM jackets is marginally affected from their exposure to high temperatures, namely from 100 °C to 150 °C and 250 °C, respectively.
- For TRM strengthened members tested at high temperature, the denser geometry in the carbon textile is more effective in shear strengthening of concrete members.
- Both non-anchored and anchored U-wrapped TRM jackets applied at full-scale T-beams remained very effective at high temperature. The shear capacity increase of non-anchored TRM jacket decreased by 30.5% due to its exposure at 150 °C, whereas the failure mode was not affected. The use of anchors increased the effectiveness of the TRM jacket by 80% despite the pull-out of anchors due to adhesive bond failure caused from the high temperature.

The above conclusions should be treated carefully as they are based on limited number of specimens. In this respect, future research should be directed towards investigating a wide range of parameters including: exposure to temperatures above 250 °C, exposure to fire, development of fire-resistant cement-based mortars and a wide variety of TRM reinforcement ratios; in order to increase the level of confidence, allowing for the development of reliable design models.

Acknowledgements

The authors wish thank the technical staff Tom Buss, Mike Langford, Nigel Rook, Balbir Loyla, Gary Davies, Sam Cook, Luke Bedford, the post-doctoral research associate Lampro Kouta and the PhD candidate Saad Raoof at the University of Nottingham for their assistance to the experimental work. The research described in this paper has been financed by the UK Engineering and Physical Sciences Research Council (EP/L50502X/1).

Notation

E_f	Modulus of elasticity of the fibres
V_f	Contribution of strengthening to the shear capacity of the beam
$V_f^{A.T.}$	Contribution of strengthening to the shear capacity of the beam at ambient temperature
$V_f^{H.T}$	Contribution of strengthening to the shear capacity of the beam at high temperature
b_w	Width of the beam
d	Effective depth of the section
h_s	Depth of the slab
k	Stress reduction factor due to high temperature
n_ℓ	Number of TRM layers
t	Nominal thickness of the textile
ρ_f	Geometrical reinforcement ratio of the composite material
σ_{eff}	Effective stress
$\sigma_{eff,high}$	Effective stress of specimens tested at high temperature

References

[1] Kodur VKR, Bisby LA, Green MF. FRP retrofitted concrete under fire conditions. J Concr Int 2006;28(12):37–44.
[2] Kodur VKR, Bisby LA, Green M. Experimental evaluation of the fire behaviour of insulated fibre-reinforced-polymer-strengthened reinforced concrete columns. Fire Saf J 2006;41(7):547–57.
[3] Firmo JP, Correia JR, Bisby LA. Fire behaviour of FRP-strengthened reinforced concrete structural elements: a state-of-the-art review. J Compos Part B Eng 2015;80:198–216.
[4] Triantafillou TC, Papanicolaou CG. Shear strengthening of reinforced concrete members with textile reinforced mortar (TRM) jackets. Mater Struct 2006;39(1):93–103.
[5] Bournas DA, Lontou PV, Papanicolaou CG, Triantafillou TC. Textile-reinforced mortar versus fibre-reinforced polymer confinement in reinforced concrete columns. ACI Struct J 2007;104(6).
[6] Carloni C, Bournas DA, Carozzi FG, D'Antino T, Fava G, Focacci F, et al. Fiber reinforced composites with cementitious (inorganic) matrix. Chapter 9. In: Pellegrino C, Sena-Cruz J, editors. Design procedures for the use of composites in strengthening of reinforced concrete structures – state of the art report of the RILEM TC 234-DUC, vols. 349–391. Springer; 2015. p. 501 [RILEM STAR Book Series].
[7] D'Antino T, Sneed LH, Carloni C, Pellegrino C. Influence of the substrate characteristics on the bond behavior of PBO FRCM-concrete joints. Constr

Build Mater 2015;30(101):838–50.
[8] Raoof SM, Koutas LN, Bournas DA. Bond between textile-reinforced mortar (TRM) and concrete substrates: experimental investigation. Compos Part B 2016;98:350–61. http://dx.doi.org/10.1016/j.compositesb.2016.05.041.
[9] Bournas DA, Pavese A, Tizani W. Tensile capacity of FRP anchors in connecting FRP and TRM sheets to concrete. Engin Struct 2015;82(1):72–81.
[10] Bournas DA, Triantafillou TC, Zygouris K, Stavropoulos F. Textile-reinforced mortar versus FRP Jacketing in seismic retrofitting of RC columns with continuous or Lap-spliced deformed bars. J Comp Constr 2009;13(5):360–71.
[11] Bournas DA, Triantafillou TC. Bond strength of lap-spliced bars in concrete confined with composite jackets. J Comp Constr 2011;15(2):156–67.
[12] Bournas DA, Triantafillou TC. Bar buckling in RC columns confined with composite materials. J Comp Constr 2011;15(3):393–403.
[13] Jesse F, Weiland S, Curbach M. Flexural strengthening of RC structures with textile-reinforced concrete. Am Concr Inst 2008;250:49–58. Special Publication.
[14] Elsanadedy HM, Almusallam TH, Alsayed SH, Al-Salloum YA. Flexural strengthening of RC beams using textile reinforced mortar–Experimental and numerical study. J Comp Struct 2013;97:40–5.
[15] Koutas L, Bournas DA. Flexural strengthening of two-way RC slabs with textile-reinforced mortar: experimental investigation and design equations. J Compos Constr 2016. http://dx.doi.org/10.1061/(ASCE)CC.1943-5614.0000713.
[16] Al-Salloum YA, Siddiqui NA, Elsanadedy HM, Abadel AA, Aqel MA. Textile-reinforced mortar versus FRP as strengthening material for seismically deficient RC beam-column joints. J Comp Constr 2011;15(6):920–33.
[17] Bournas DA, Triantafillou TC. Biaxial bending of RC columns strengthened with externally applied reinforcement combined with confinement. ACI Struct J 2013;110(2):193–204.
[18] Koutas LN, Bousias SN, Triantafillou TC. Seismic strengthening of masonry-infilled RC frames with TRM Experimental study. J Comp Constr 2015;19(2): 04014048. http://dx.doi.org/10.1061/(ASCE)CC.1943-5614.0000507.
[19] Bournas DA. Strengthening of existing structures: selected case studies. In: Triantafillou TC, editor. Textile fibre composites in civil engineering, (Ch. 17). Elsevier, Woodhead Publishing Limited; 2016. p. 389–411. http://dx.doi.org/10.1016/B978-1-78242-446-8.00018-5.
[20] Brückner A, Ortlepp R, Curbach M. Anchoring of shear strengthening for T-beams made of textile reinforced concrete (TRC). Mater Struct 2008;41(2): 407–18.
[21] Azam R, Soudki K. FRCM strengthening of shear-critical RC beams. J Comp Constr 2014;18(5):04014012. http://dx.doi.org/10.1061/(ASCE)CC.1943-5614.0000464.
[22] Tzoura E, Triantafillou TC. Shear strengthening of reinforced concrete T-beams under cyclic loading with TRM or FRP jackets. Mater Struct 2014. http://dx.doi.org/10.1617/s11527-014-0470-9.
[23] Tetta ZC, Koutas LN, Bournas DA. Textile-reinforced mortar (TRM) versus fibre-reinforced polymers (FRP) in shear strengthening of concrete beams. Compos Part B 2015;77:338–48. http://dx.doi.org/10.1016/j.compositesb.2015.03.055.
[24] Loreto G, Babaeidarabad S, Leardini L, Nanni A. RC beams shear-strengthened with fabric-reinforced-cementitious-matrix (FRCM) composite. Int J Adv Struct Eng (IJASE) 2015:1–12.
[25] Ombres L. Structural performances of reinforced concrete beams strengthened in shear with a cement based fibre composite material. Comp Struct 2015;122:316–29.
[26] Tetta ZC, Koutas LN, Bournas DA. Shear strengthening of full-scale RC T-beams using textile-reinforced mortar and textile-based anchors. Compos Part B 2016;95:225–39. http://dx.doi.org/10.1016/j.compositesb.2016.03.076.
[27] Colombo I, Colombo M, Magri A, Zani G, di Prisco M. Textile reinforced mortar at high temperatures. Appl Mech Mater 2011;82:202–7.
[28] Al-Salloum YA, Almusallam TH, Elsanadedy HM, Iqbal RA. Effect of elevated temperature environments on the residual axial capacity of RC columns strengthened with different techniques. Constr Build Mater 2016;115: 345–61.
[29] Bisby L, Stratford T, Hart C, Farren S. Fire performance of well-anchored TRM, FRCM and FRP flexural strengthening systems. Adv Compos Constr 2013. Network Group for Composites in Construction, Belfast, UK.
[30] 1015-11 EN. Methods of test for mortar for masonry – Part 11: determination of flexural and compressive strength of hardened mortar. Brussels: Comité Européen de Normalisation; 1993.
[31] Koutas LN, Pitytzogia A, Triantafillou TC, Bousias SN. Strengthening of infilled reinforced concrete frames with TRM: study on the development and testing of textile-based anchors. J Compos Constr 2014;18(3). http://dx.doi.org/10.1061/(ASCE)CC.1943-5614.0000390.
[32] Pellegrino C, Vasic M. Assessment of design procedures for the use of externally bonded FRP composites in shear strengthening of reinforced concrete beams. Compos Part B 2013;45(1):727–41.
[33] Rousakis T, Saridaki M, Mavrothalassitou S, Hui D. Utilization of hybrid approach towards advanced database of concrete beams strengthened in shear with FRPs. Compos Part B 2016;85:315–35.